Hydrological Sciences Journal

ISSN: 0262-6667 (Print) 2150-3435 (Online) Journal homepage: https://www.tandfonline.com/loi/thsj20

Water resources and climate change impact modelling on a daily time scale in the Peruvian Andes

Norina Andres, Fernando Vegas Galdos, Waldo Sven Lavado Casimiro & Massimiliano Zappa

To cite this article: Norina Andres, Fernando Vegas Galdos, Waldo Sven Lavado Casimiro & Massimiliano Zappa (2014) Water resources and climate change impact modelling on a daily time scale in the Peruvian Andes, Hydrological Sciences Journal, 59:11, 2043-2059, DOI: 10.1080/02626667.2013.862336

To link to this article: https://doi.org/10.1080/02626667.2013.862336

Accepted author version posted online: 12 Nov 2013.
Published online: 23 Sep 2014.

Hydrological Sciences Journal – Journal des Sciences Hydrologiques, 59 (11) 2014
http://dx.doi.org/10.1080/02626667.2013.862336

Water resources and climate change impact modelling on a daily time scale in the Peruvian Andes

Norina Andres[1], Fernando Vegas Galdos[2], Waldo Sven Lavado Casimiro[3] and Massimiliano Zappa[1]

[1]*Swiss Federal Institute for Forest, Snow and Landscape Research (WSL), CH-8903 Birmensdorf, Switzerland*
norina.andres@wsl.ch

[2]*Universidad de Cantabria, Departamento de Ciencias y Técnicas del Agua y del Medio Ambiente, Santander, Spain*

[3]*Servicio Nacional de Meteorología y Hidrología del Perú (SENAMHI), Lima, Perú*

Received 6 September 2012; accepted 12 September 2013; open for discussion until 1 May 2015

Editor Z.W. Kundzewicz; **Associate editor** D. Gerten

Abstract Estimating water resources is important for adequate water management in the future, but suitable data are often scarce. We estimated water resources in the Vilcanota basin (Peru) for the 1998–2009 period with the semi-distributed hydrological model PREVAH using: (a) raingauge measurements; (b) satellite rainfall estimates from the TRMM Multi-satellite Precipitation Analysis (TMPA); and (c) ERA-Interim re-analysis data. Multiplicative shift and quantile mapping were applied to post-process the TMPA estimates and ERA-Interim data. This resulted in improved low-flow simulations. High-flow simulations could only be improved with quantile mapping. Furthermore, we adopted temperature and rainfall anomalies obtained from three GCMs for three future periods to make estimations of climate change impacts (Delta-change approach) on water resources. Our results show more total runoff during the rainy season from January to March, and temporary storages indicate that less water will be available in this Andean region, which has an effect on water supply, especially during dry season.

Key words TRMM, TMPA; climate change anomalies; ERA-Interim; hydrological modelling; Taylor diagram; quantile mapping; Peru

Modélisation de ressources en eau et impact du changement climatique sur une échelle de temps journalier dans les Andes péruviennes

Résumé Estimation des ressources en eau est importante pour la gestion adéquate de l'eau à l'avenir, mais les données appropriées sont souvent rares. Nous avons estimé les ressources en eau dans le bassin de Vilcanota (Pérou) pour la période 1998–2009 avec le PREVAH de modèle hydrologique semi-distribué en utilisant: (a) les mesures pluviométriques; (b) les estimations des précipitations par satellite TRMM du multi-satellite Précipitations analyse (TMPA); et (c) les données de réanalyse ERA-Interim. Changement multiplicatif et cartographie quantile ont été appliqués à post-traiter les estimations TmpA et les données de l'ERA-Interim. Cela s'est traduit par l'amélioration des simulations à faible débit. Simulations de haut-débit ne pouvaient être améliorées avec la cartographie quantile. En outre, nous avons adopté la température et des précipitations anomalies obtenues à partir de trois MCG pour trois périodes futures de faire des estimations des impacts du changement climatique (Delta-changement d'approche) sur les ressources en eau. Nos résultats montrent ruissellement plus total au cours de la saison des pluies de Janvier à Mars, et les stockages temporaires indiquent que moins d'eau sera disponible dans la région andine, qui a un effet sur l'approvisionnement en eau, en particulier pendant la saison sèche.

Mots clefs TRMM, TMPA ; changement climatique anomalies ; ERA-Interim ; modélisation hydrologique ; Taylor schéma ; cartographie quantile ; Pérou

1 INTRODUCTION

In the context of climate change, water management has become increasingly significant, especially in mountainous regions which depend on water contributions from glaciers (Viviroli *et al.* 2011) and páramos. Páramos consist of a collection of neotropical alpine grassland ecosystems covering the upper region of the northern Andes (Buytaert *et al.* 2006). Estimating water resources is therefore important for adequate water management in the future. Here,

hydrological models, driven by meteorological data, can provide useful information for decision making. However, access to ground-based meteorological measurements is often difficult, especially in mountainous regions like the Andes, where few data are available (Schwarb *et al.* 2011).

Satellite-based precipitation estimates are a potential alternative source of forcing data for hydrological modelling, since they cover a large area with a high temporal and spatial resolution (Su *et al*. 2008). In recent years, several satellite-based products have been developed (Tobin and Bennett 2010), including the Tropical Rainfall Measuring Mission (TRMM) Multi-satellite Precipitation Analysis (TMPA, Huffman *et al.* 2007). TMPA estimates have been applied in hydrological modelling all over the world (e.g. Collischonn *et al*. 2008, Lavado Casimiro *et al.* 2009, Wagner *et al.* 2009, Pan *et al*. 2010, Tobin and Bennett 2010, Jiménez *et al*. 2011, Bitew *et al.* 2012). Lavado Casimiro *et al.* (2009) used on-site rainfall data to improve monthly TMPA estimates (3B43 product) for two basins in Peru, and linked them to a water balance model with monthly resolution. The improved data appeared to describe the hydrological regimes well. Su *et al.* (2008) applied the variable infiltration capacity (VIC) semi-distributed hydrological model to the La Plata basin in South America. Their simulations with TMPA estimates were able to capture the daily flood events well, but tended to overestimate most flood peaks. Furthermore, seasonal and inter-annual streamflow variability was well reproduced. The analysis by Su *et al.* (2008) demonstrated the potential of TMPA products for hydrological forecasting in data-sparse regions. Collischonn *et al.* (2008) found that raingauge data gave better simulation results than TMPA estimates in the Tapajós River basin, Brazil.

Other alternative sources of forcing data for hydrological modelling are re-analysis products, which are developed by reprocessing historical, observational data using a consistent modern analysis system. One example is the global atmospheric re-analysis product ERA-Interim (Berrisford *et al.* 2009).

The quantification of the effect of climate change on hydrological components within a catchment is valuable for future planning within the water sector (Laghari *et al*. 2012). In recent years, interest in climate change modelling has grown. In the Fourth Assessment Report of the Intergovernmental Panel on Climate Change (IPCC 2007), general circulation models (GCMs) were used to give an overview of the current situation and provide projections of possible changes in climate (Ardoin-Bardin *et al.* 2009). The modelling of the climatic system is very complex and the climate projections are not easy to incorporate into hydrological impact studies (Allen and Ingram 2002, Ardoin-Bardin *et al*. 2009). One problem with GCMs is that the climate models differ (IPCC 2001a, Ardoin-Bardin *et al*. 2009), especially for precipitation (Dai 2006). However, using a range of models can also be an advantage, for example to sample potential uncertainty in the initial conditions and also in future projections (Randall *et al.* 2007). Furthermore, the resolution of the climate models is often too coarse, compared to that of hydrological modelling (IPCC 2001a, Ardoin-Bardin *et al*. 2009). Regional climate models operate at higher resolution and often with more detailed topography and physical parameterizations (IPCC 2001b); GCMs are not perfect, but they are still a powerful tool for assessing climate change (Ardoin-Bardin *et al*. 2009).

General circulation models have been used for several studies of the impact of climate change on water resources in several regions of the world. Lavado Casimiro *et al.* (2011) assessed the climate change impacts on the hydrology of the Peruvian Amazon-Andes basin by combining the outputs of three GCMs with two hydrological models with monthly resolution. Buytaert *et al*. (2009) found a wide divergence in simulated monthly discharge for catchments in south Ecuador that were driven by different GCM forcing data. Vergara *et al*. (2011) simulated flows for the 2050–2059 period in the Santa River basin in Peru and found monthly discharges were projected to decrease throughout the year in comparison with observed historical values.

Since the Andean region of Peru is so vulnerable to climate change (Bradley *et al.* 2006), the Peruvian Ministry of the Environment, in collaboration with the Swiss Agency for Development and Cooperation (SDC), initiated a programme on climate change adaptation (PACC; *Programa de Adaptación al Cambio Climático*) in the regions of Cuzco and Apurimac. The programme integrates water management, disaster prevention and food security. In order to support planning and resource management decisions that can guarantee a continuity of both water resources and development, it is imperative to quantify the current water resources and analyse the possible effects of climate changes. However, data on the Peruvian Andes are very limited (Salzmann *et al.* 2009) and, in the region of the Vilcanota basin (VB) in Peru, for example, little experience on estimating water resources on a daily time scale was found.

Studies with TMPA estimates, ERA-Interim and GCM data have already been done. Compared to

these our focus lies on the presentation of alternative data sources for hydrological studies to estimate water resources, especially when few data are available. We also use two approaches of different complexity in order to post-process TMPA and ERA-Interim data and evaluate such methods with respect to the estimation of water resources. We introduce three data sources which are available for the Vilcanota basin in the high mountains of Peru and demonstrate how they can be used for hydrological modelling, including the application of climate impact scenarios and yield information on water resources for the target region. Another objective is to test for the first time the performance of the hydrological model PREVAH (Precipitation-Runoff-EVApotranspiration Hydrotope; Viviroli *et al.* 2009a) for the study region, with the focus on simulations at a daily time scale.

After introducing the study area, data and methods, we first compare the results of the PREVAH hydrological model (forced with daily TMPA estimates, ERA-Interim data and raingauge data) with stream gauge data; and second, we evaluate the impact of climate change on the daily hydrology by forcing the hydrological model with outputs of three GCMs, yielding impact scenarios for three future periods.

2 STUDY AREA AND DATA

2.1 Study area

The study area is in the southern Peruvian Andes within the Vilcanota basin (VB), which is a tributary of the Amazon River system (Fig. 1). The catchment has an area of 9160 km^2, belongs to the administrative division of Cuzco and is characterized by the presence of glaciers, steep slopes and an elevation range of 2160–6290 m a.s.l. Ecosystem complexes like páramos and puna (Sánchez-Vega and Dillon 2006) play an important role in the dynamics of the highland tributary system. Páramos exist above the upper treeline and below the permanent snowline, and have high humidity, low temperatures and a high vegetation coverage. Puna, in contrast, have lower humidity, a lower vegetation coverage and an active vegetation season of only 5 months (Sánchez-Vega and Dillon 2006).

Predominant soil types in the study area are Lithosols and Kastanozems (FAO-UNESCO 1988). Land cover/land use in VB is directly related to the altitude, the prevailing climate and soil type. The land cover is dominated by natural grassland (82.7%), shrublands (10.4%), scattered areas of traditional cultivation (1.7%), and small glaciers and lakes (1.4%). Agriculture occurs predominantly in the inter-Andean valleys. The rural population practices agricultural production, most of them being small-scale farmers and livestock owners. The principal urban area in VB is the city of Cuzco, where around 32.7% of the population in the study area is concentrated (INEI 2011).

Recent years have seen some extreme hydrological events in VB, such as the 2010 flood (Lavado Casimiro *et al.* 2010). A Tropical South rainfall regime is predominant in VB (Villar *et al.* 2009), with a rainy season between December and April,

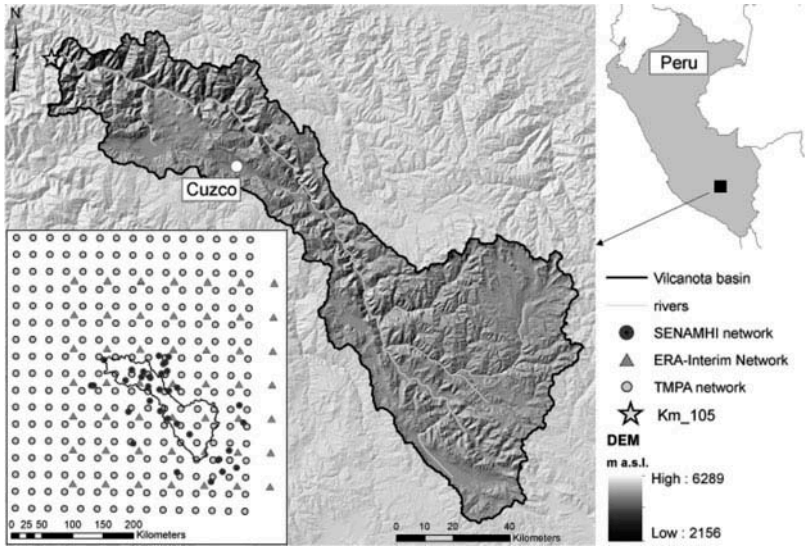

Fig. 1 Study area and data network.

and a dry season between May and November. From 1998 to 2009 the average annual precipitation was 777 mm year^{-1}, with considerable variability between years, which is connected with the sea surface temperature in the tropical Atlantic Ocean and the Southern Oscillation Index of the Pacific Ocean (Lavado Casimiro *et al.* 2012). Generally, during El Niño, droughts are observed in this region, while La Niña is associated with heavy rain spells.

2.2 Available data

2.2.1 Ground station data A data portal with historical climatic data collected from more than 100 stations of the Peruvian Meteorological and Hydrological Service (SENAMHI) around Cuzco was established as part of the PACC program (see also Schwarb *et al.* 2011). Thirty-six (36) stations were selected from this data portal. They contained homogenized daily data on temperature, precipitation and relative humidity for the years 1960–2009 (see Table 1).

Daily discharge data for 1980–2009 were available for calibration from a streamgauge which gauges the Vilcanota River close to Machu Picchu (Km_105); these data are for a stable profile section. The station belongs to a private hydropower company (EGEMSA).

2.2.2 TMPA estimates (TRMM 3B42 V6) The TRMM 3B42 Research Version 6 product combines measurements of different space-borne sensors and gauge data at fine scales. These data consist of hourly precipitation estimates (mm h^{-1}), and are available with a 3-h temporal and 0.25° × 0.25° spatial resolution. Data had been collected since 1998 and coverage lies between 50°N and 50°S (Huffman *et al.* 2007, Scheel *et al.* 2011).

The TRMM product, 3B42 V6, is a merged dataset that takes advantage of the best available data. The product is a combination of passive microwave (PMW) and infrared (IR) precipitation estimates from a variety of satellite platforms (TRMM; the Defense Meteorological Satellite Program, DMSP; the Aqua mission and National Oceanic and Atmospheric Administration, NOAA; Huffman *et al.* 2007). The PMW coverage gaps are filled with high-quality, calibrated infrared data (Tobin and Bennett 2010). The TMPA data are available in real time and as a post-processed research product. The research product is merged with ground station data and is computed about 15 days after the end of each month (Huffman *et al.* 2007, Su *et al.* 2008). In this study we used the TRMM 3B42 V6 product (henceforth called TMPA estimates) for the period 1998–2009.

Several studies have been implemented to validate the quality of the precipitation estimates of this product. In the Central Andes, Scheel *et al.* (2011) tested the dependency of the estimate performance on changing spatial and temporal resolutions. They found large biases in the estimation of daily precipitation amounts. The correlation with ground data increased strongly with temporal aggregation, but the change in spatial aggregation did not reveal any significant changes in correlation coefficient and estimate performance. Su *et al.* (2008) found similar results for the La Plata Basin in South America. The TMPA estimates agreed well with gauge data on a monthly time scale, but the agreement was reduced on a daily time scale, especially for high rainfall rates.

2.2.3 ERA-Interim ERA-Interim is a reanalysis of the global atmosphere and surface

Table 1 Overview of available meteorological data and their interpolation, further processing and available time period. P: precipitation; T: temperature; RH: relative humidity; S: sunshine duration; and W: wind speed. Available data interpolated with inverse distance weighting (IDW) are displayed in **bold**, those interpolated with detrended inverse distance weighting (DIDW) are in *italic* and those with lapse rate (LPR) are underlined.

	Ground station data	TMPA	ERA-Interim	GCM
Available data	**P**, *T, RH*	**P**	**P**, T, **RH, S, W**	T, P
Time resolution	Daily	3 h and daily	Daily	Monthly
Interpolation to grid	**IDW**, *DIDW*; 540-m resolution	**IDW**; 540-m resolution	**IDW**, LPR; 540-m resolution	Kriging (0.25° × 0.25° resolution)
Further processing	Averaged to meteorological sub-units	Averaged to meteorological sub-units	Averaged to meteorological sub-units	Delta-change approach
Available time period	1960–2009	1998–2009	1998–2009	CC scenarios 2010–2039, 2040–2069, 2070–2100

conditions covering the data-rich period from 1979 to the present (Berrisford *et al*. 2009) by the European Centre for Medium-Range Weather Forecasts (ECMWF). This dataset provides a multivariate, spatially complete and coherent record for the global atmospheric circulation. Gridded data products include a large variety of 3-hourly surface parameters and 6-hourly upper-air parameters (Dee *et al.* 2011). We obtained from ECMWF gridded precipitation, sunshine duration and wind speed data at a daily resolution for the period 1998–2009. The precipitation data had been tested and compared with other datasets, for example by Lorenz and Kunstmann (2012). They found an overestimation of rainfall over the Andes of up to 2.5 mm d^{-1}.

2.2.4 General circulation model (GCM) outputs To evaluate the potential future impact of climate change in VB, precipitation and temperature outputs from GCMs of the IPCC Fourth Assessment Report were coupled with the hydrological model PREVAH. In this study, we used the following GCMs: the BCM2 model (Bjerkness Centre for Climate Research, Norway) with a resolution of 1.9° × 1.9°; the CSMK3 model (Commonwealth Scientific and Industrial Research Organisation, CSIRO, Atmospheric Research, Australia) with a resolution of 1.9° × 1.9°; and the MIHR model (Center for Climate System Research, University of Tokyo, National Institute for Environmental Studies, and Frontier Research Center for Global Change, JAMSTEC, Japan) with a resolution of 1.1° × 1.1° (Semenov and Stratonovitch 2010). We chose these three models because they have a resolution below 2° and are available for the two emissions scenarios A1B and B1 (see below), and because they were already used by Lavado Casimiro *et al.* (2011) to assess the impact of climate change on the hydrology in two Peruvian Amazon-Andes basins on a monthly scale. We are aware that the whole range of possible climate change output is not covered by choosing only these three GCMs, but the exploration of more GCMs was outside the scope of this study, being focused on different data sources to obtain daily hydrological time series for water resources assessment in the target area.

Two scenarios were chosen from the Special Report on Emissions Scenarios (SRES) to calculate the future climate on a regional scale (2010–2100): A1B and B1 (Semenov and Stratonovitch 2010). The period 1965–1999 (called 'the climate of the 20th century') was used to calculate the monthly anomalies (Delta-change approach) in precipitation and temperature. Monthly mean precipitation and temperature data for each GCM, emissions scenario and time period (climate of the 20th century 1965–1999, 2010–2039, 2040–2069, 2070–2100) were obtained from the IPCC Distribution Centre (http://www.ipcc-data.org). These data were spatially interpolated to 0.25° × 0.25° over our study region using the kriging methodology (Oliver and Webster 1990, Lavado Casimiro *et al.* 2011) (see Table 1).

2.2.5 Physiographical information Digital elevation data were obtained from the Shuttle Radar Topography Mission (SRTM) with a resolution of three arc seconds, soil information from the FAO Soil Map of the World (FAO-UNESCO 1988, Menzel 1996), and information on land use from the MODIS Land Cover (MOD12Q1) product (Friedl *et al.* 2002). Both meteorological and physiographic data were pre-processed using a suite of tools included in PREVAH (Viviroli *et al.* 2009a).

3 MODEL AND METHODOLOGY

3.1 Hydrological model PREVAH

The semi-distributed model PREVAH (Precipitation-Runoff-EVApotranspiration Hydrotope, Viviroli *et al.* 2009a) was selected for the hydrological simulations because it has the ability to describe and accurately represent the heterogeneity of mountainous, hydrological systems with highly variable environmental and climatic conditions. The PREVAH model was developed by the Institute of Geography at the University of Bern (GIUB), the Swiss Federal Institute for Forest, Snow and Landscape Research (WSL) and the Institute for Atmospheric and Climate Science ETH Zürich (IACETH), Switzerland. The PREVAH model has been applied to investigate water resources in mountainous basins (Zappa and Kan 2007, Kobierska *et al.* 2013) in poorly gauged areas of China (Bosshard and Zappa 2008) and Russia (Oltchev *et al.* 2002), and also as a source of hydrological indicators for estimating climate change impacts on vegetation distribution (Randin *et al.* 2009). A review of selected application examples for PREVAH is presented in Viviroli *et al*. (2009a), which also provides an overview of the model basics, calibration and pre- and post-processing tools.

3.1.1 Model parameterization Three types of input data are required to run PREVAH: (a) meteorological input: air temperature, precipitation, relative humidity, global radiation, wind speed and sunshine duration in hourly or daily time steps, (b) physiographical information for the hydrological response units (HRUs), and (c) a control file with the configuration of the tuneable model parameters that control the individual sub-models. These parameters need to be calibrated to adjust the model to the conditions at the study site (Viviroli *et al.* 2009a).

The spatial and temporal resolutions to run the model were selected according to the availability of data. In this study, a spatial resolution of 540 m was selected, according to previous studies about the critical resolution for hydrological modelling dependent on catchment size (Zappa 2002); 1-day time steps were selected as the final resolution for all input and output data. Physiographical information was clustered into HRUs to summarize the grid cells for those areas in the basin in which similar hydrological behaviour could be expected. Each HRU was described with a set of parameters based on information derived from the digital elevation model, soil maps, land use and land surface characteristics (Viviroli *et al.* 2009a). The soil depth and plant available field capacity were determined from soil classes contained in the FAO Soil Map of the World (FAO-UNESCO 1988), as described in (Viviroli *et al.* 2009a, Viviroli *et al.* 2007).

The inverse distance weighting (IDW), the detrended inverse distance weighting (DIDW) and lapse rate (LPR) methods were used to obtain gridded meteorological data with a spatial resolution of 540 m (Viviroli *et al.* 2009a) using the available set of ground station, TMPA and ERA data (see Table 1). The spatially interpolated meteorological information is averaged for previously defined meteorological subunits (Viviroli *et al.* 2009a).

3.2 PREVAH calibration and validation

An automatic calibration procedure was applied to adjust the tuneable parameters, and thus the model, to the conditions prevailing in the specific catchment. The model was calibrated for three different precipitation datasets: The raingauge data, the TMPA estimates and the ERA-Interim data. The model was calibrated by maximizing the agreement between the observed (Km_105) and simulated hydrographs, which involved selecting a suitable set of tuneable parameters. The tuneable parameters can be subdivided into five families (precipitation, snowmelt, soil moisture recharge, runoff formation and, optionally, ice melt), which control the sub-models within PREVAH. The most sensitive tuneable parameters are the adjustment factors for snowfall and rainfall (Viviroli *et al.* 2009a), the parameters controlling the snowmelt module (Zappa *et al.* 2003), the soil moisture recharge (Zappa and Gurtz 2003), the runoff generation module (Gurtz *et al.* 2003) and the glacier melt module (Koboltschnig *et al.* 2008). Selection of parameter values occurs within a prescribed parameter space (originally defined by physical considerations and experience). The acceptable parameter space can be edited by the user (Viviroli *et al.* 2007). The automatic calibration approach was first presented in Zappa and Kan (2007) and is explained in more detail in Viviroli *et al.* (2009a). The period 1999–2004 was selected for calibration, and the period 2005–2009 for validation. The first year (1998) was defined as a 'spin up' (Viviroli *et al.* 2009b). In particular, it serves to fill the low-frequency storages for baseflow and snow. The results from this year were therefore discarded and not used for the evaluation of the model performance. The following statistical criteria were used to evaluate the calibration results: the Nash and Sutcliffe efficiency coefficient (NS), the Nash and Sutcliffe logarithmic coefficient (NSL) and the absolute bias (VOL, mm):

$$\mathrm{NS} = 1 - \left(\frac{\sum_{i=1}^{N} (Q_{\mathrm{obs}} - Q_{\mathrm{sim}})^2}{\sum_{i=1}^{N} (Q_{\mathrm{obs}} - \overline{Q_{\mathrm{obs}}})^2} \right) \tag{1}$$

$$\mathrm{NSL} = 1 - \left(\frac{\sum_{i=1}^{N} (\ln Q_{\mathrm{obs}} - \ln Q_{\mathrm{sim}})^2}{\sum_{i=1}^{N} (\ln Q_{\mathrm{obs}} - \ln \overline{(Q_{\mathrm{obs}})})^2} \right) \tag{2}$$

$$\mathrm{VOL} = \sum_{i=1}^{N} (Q_{\mathrm{sim}} - Q_{\mathrm{obs}}) \tag{3}$$

where Q is the simulated (sim) or observed (obs) discharge (mm d^{-1}).

3.3 Hydrological modelling with TMPA and ERA-Interim data

By comparing the precipitation data of the TMPA estimates and ERA-Interim with the basin averaged interpolation of raingauge data, we found an underestimation of rainfall for the TMPA estimates and a

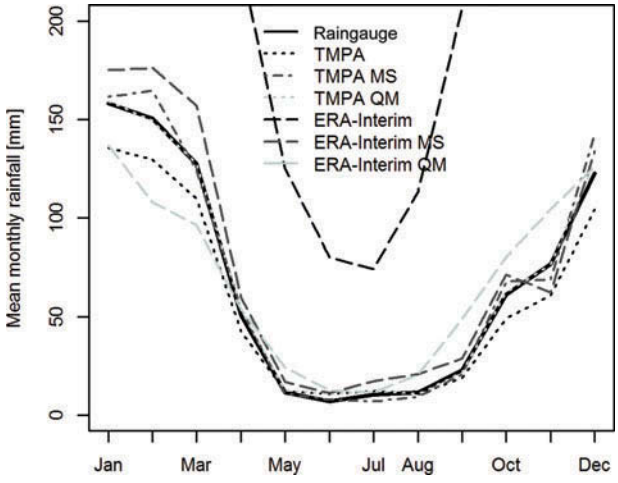

Fig. 2 Mean monthly rainfall (mm) of raingauges, TMPA estimates and ERA-Interim data (1998–2009). Two simple post-processing methods, a multiplicative shift (MS) and quantile mapping (QM) were used to correct the absolute bias of TMPA and ERA-Interim precipitation data.

very large overestimation for the ERA-Interim data (see Fig. 2). Bias correction is a current state of research and discussion (Ehret *et al.* 2012). Here, we applied two different bias correction techniques to compensate for this under- and overestimation (straight multiplicative shift and quantile mapping).

Using the multiplicative shift method, we compared daily precipitation data measured by raingauges with the TMPA estimates and ERA-Interim data for the years 1998–2009 and calculated the mean monthly differences (see Table 2). The differences from 1999 to 2004 were used to calibrate the datasets with a multiplicative shift (here explained for the TMPA estimates):

$$R_C = R_{\mathrm{TMPA},i} * \frac{\overline{R_{\mathrm{obs}}}}{\overline{R_{\mathrm{TMPA}}}} \quad (4)$$

where R_C is the post-processed TMPA estimate on day *i*, $R_{\mathrm{TMPA},i}$ is the TMPA estimate on day *i*, and $\overline{R_{\mathrm{obs}}}$ and $\overline{R_{\mathrm{TMPA}}}$ are the long-term monthly means of the raingauge data and TMPA estimates for a given month. The years 2005–2009 were chosen for the validation.

The second post-processing method we applied is quantile mapping (QM). This method originates from the empirical transformation of Panofsky and Brier (1968) and is based on daily constructed empirical cumulative distribution functions (ecdf) of modelled and observed datasets; in our case the TMPA estimates (or ERA-Interim data) and the raingauge data. The aim of this method is to translate the TMPA estimates (or ERA-Interim data) into a plausible range with respect to the dataset relying on interpolated raingauge data. For each day, we estimated the quantile of the daily precipitation of the TMPA estimates (or ERA-Interim data) in the corresponding ecdf and substituted this value with the same quantile in the corresponding ecdf of the raingauge data. To get a better approximation, we calibrated each year independently with the remaining years by using the ecdf of the calibration year of the TMPA estimates (or ERA-Interim data) and the ecdf of the remaining years of the raingauge data. For example, we built the ecdf for the year 1998 of the TMPA estimates and the ecdf for the years 1999–2009 of the raingauge data and then applied then the QM method. The advantage of the QM technique is that no new extremes can be obtained (Jakob Themeßl *et al.* 2011) and that the spatial distribution of the rainfall amount is preserved.

The hydrological model PREVAH was then forced with the raingauge-derived estimates, the original and post-processed TMPA estimates and the ERA-Interim data for VB. Simulations with post-processed TMPA and ERA-Interim precipitation forcing were performed using the tuneable model parameters obtained by calibrating PREVAH with raingauge forcing (see Section 3.2). By removing the bias of TMPA and ERA with respect to the raingauge forcing, we also assumed that we need to adopt the same scaling of precipitation as estimated for simulations driven by raingauge data. The simulation results were compared with the observed daily discharge at the streamgauge Km_105, and statistically assessed. In addition, Taylor diagrams were used to test how well the simulations and

Table 2 Monthly factor of correction, based on long-term monthly mean rainfall (1998–2004) of raingauge data (R_{obs}), TMPA estimates (R_{TMPA}) and ERA-Interim data ($R_{\mathrm{ERA\text{-}Interim}}$).

	Jan	Feb	Mar	Apr	May	Jun	Jul	Aug	Sep	Oct	Nov	Dec
$\overline{R_{\mathrm{obs}}}/\overline{R_{\mathrm{TMPA}}}$	1.19	1.27	1.13	1.26	0.86	0.64	0.51	0.81	1.07	1.38	1.13	1.36
$\overline{R_{\mathrm{obs}}}/\overline{R_{\mathrm{ERA-Interim}}}$	0.36	0.46	0.44	0.26	0.13	0.12	0.21	0.17	0.14	0.23	0.16	0.29

measurements match each other in terms of their correlation, root mean square difference and the ratio of their variances (see Taylor 2001).

3.4 Hydrological modelling of climate change scenarios

The performance of the three GCMs was tested by comparing monthly temperature and precipitation for the GCM climate of the 20th century (1965–1999) with observed data from Lavado Casimiro *et al.* (2011). The CSMK3 model performed best, but R values were very high for all models except for the BCM2 model for rainfall (see Table 3).

The following Delta-change approach (Gleick 1986, Graham *et al.* 2007, Bosshard *et al.* 2011) was adopted to multiply or add the monthly changes to the observed datasets for the period 1991–2009:

$$P_{\mathrm{SCEN}}(t) = P_{\mathrm{OBS}}(t) * \Delta P(\mathrm{SCEN_{ID}}) \quad (5)$$

$$T_{\mathrm{SCEN}}(t) = T_{\mathrm{OBS}}(t) + \Delta T(\mathrm{SCEN_{ID}}) \quad (6)$$

The relative monthly change of two GCM-derived climate variables (ΔP and ΔT for precipitation and temperature, respectively) between the climatology of the 20th century (1965–1999) and a future period (2010–2100) was calculated for each cell of the GCM, SRES scenario and time period, and averaged over the study region. No bias correction of the raw GCM data was applied. At each time step t within the hydrological model, these monthly changes (ΔP, ΔT) were used to condition the gridded daily observed meteorological information (see Section 2.2.1) (P_{OBS} and T_{OBS}) on precipitation P (multiplicative approach) and air temperature T (additive approach). The term $\mathrm{SCEN_{ID}}$ is an identifier for the monthly-based changes; P_{SCEN} and T_{SCEN} are the values of the meteorological forcing after the modification, determined by factors obtained from the climate scenarios.

Table 3 Statistical comparison of the monthly observed data from Lavado Casimiro *et al.* (2011) and the climate of the 20th century (1965–1999) of the GCMs. B: bias (mm, °C); R: Pearson correlation coefficient (-).

GCM	Rainfall		Temperature	
	B (mm)	R (-)	B (°C)	R (-)
BCM2	−145	0.56	−3	0.87
MIHR	−189	0.83	−3	0.85
CSMK3	−74	0.79	1	0.88

This method implies that the daily variability of P_{SCEN} or T_{SCEN} within a specific month is transferred from the observed data (P_{OBS}, T_{OBS}). The use of data starting from 1993 was only possible for raingauge-based simulations. This extends the application of PREVAH beyond the periods used for calibration, verification and comparison with TMPA and ERA products.

Using the Delta-change methodology meant that the results we obtained would not be evaluated with respect to extreme events, since the variability of the meteorological input (e.g. wet-dry spells and severe precipitation events) is not changed with respect to the baseline period.

4 RESULTS AND DISCUSSION

4.1 Post-processing of TMPA and ERA-Interim data

The mean monthly differences between TMPA estimates and raingauge data from 1998–2009 (Fig. 2) show that TMPA estimates clearly underestimate rainfall from September to April and slightly overestimate rainfall from June to July. This leads to a rainfall volume deficit of –14.8% for the entire period (1998–2009). The TMPA estimates seem more suitable for this region than ERA-Interim precipitation data, because the latter greatly overestimate mean monthly rainfall during the whole year (+293%). Due to this overestimation, ERA-Interim precipitation data are *a priori* not suitable for detailed water resources assessment in our study region. Post-processing has to be applied to correct these biases.

4.1.1 Multiplicative shift The mean monthly TMPA estimates corrected with the multiplicative shift (henceforth called TMPA MS) yielded a better approximation to the raingauge data after the shift, as can be seen in Fig. 2. A slight overestimation in wet months (December–February) can be detected, but the overall performance seems to be better than with the uncorrected TMPA estimates. However, the difference in the sum of rainfall from 1998 to 2009 between the raingauge data and the TMPA estimates was reduced from –14.8% to +2.8% with the multiplicative shift. The greatly overestimated precipitation data of ERA-Interim could be corrected with the multiplicative shift (ERA-Interim MS), but still an overestimation persists (+13.96%, see Fig. 2). This could be due to the correction factor based on the chosen calibration period.

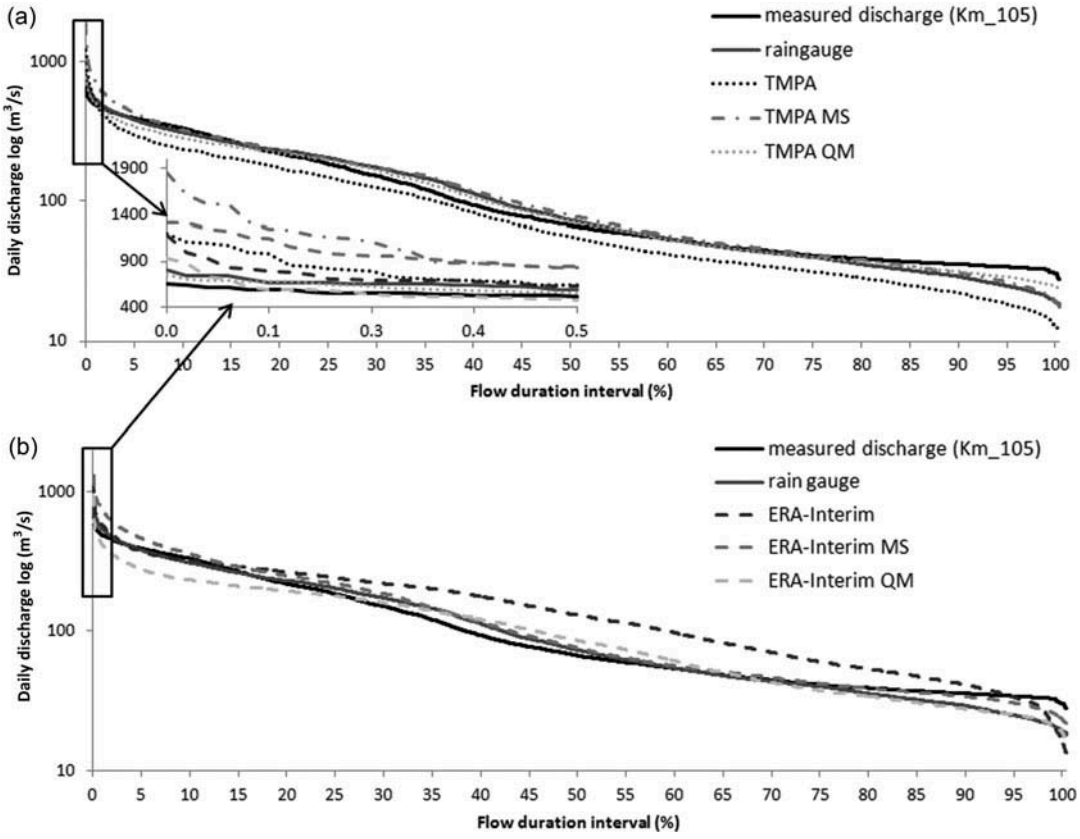

Fig. 3 Flow duration curves (1999–2009) for: (a) measured discharge and simulated raingauge data, TMPA estimates and (b) ERA-Interim data, as well as the simulation results of the post-processed (MS and QM) data. The highest 0.5% of the daily discharge is presented in the small graph.

The main limitation of the multiplicative shift technique is that the correction factor is applied to the TMPA estimates and ERA-Interim data regardless of the amount of precipitation. As a result, peak flows in particular were greatly overestimated, as demonstrated by the flow duration curves presented in Fig. 3.

4.1.2 Quantile mapping The post-processed TMPA estimates with quantile mapping (TMPA QM), shown in Fig. 2, give a very good approximation to the raingauge data (much better than TMPA MS). The difference in the sum of rainfall from 1998 to 2009 could be reduced to +0.9%. The absolute bias in precipitation of the ERA-Interim data (ERA-Interim QM) could be reduced to +0.8%, but an underestimation in mean monthly rainfall from January to March and an overestimation from May to November exist (Fig. 2).

Apart from the overestimation at the beginning of the year, ERA-Interim MS follows the monthly shape of the raingauge data curve in Fig. 2 better than ERA-Interim QM.

4.2 Hydrological modelling results with TMPA and ERA-Interim data

4.2.1 After calibration and validation The efficiency criteria of the simulation results of the calibration, validation and full application period are presented in Table 4. Simulations with raingauge data yielded better results (highest NS and NSL values and the lowest discharge absolute bias) when compared to discharge measurements than simulations with TMPA estimates. Similar outcomes have been achieved, for example, by Collischonn *et al.* (2008) and Jiménez *et al.* (2011). Generally, the high-flow periods are well captured by the TMPA estimates, but we found, as did Su *et al.* (2008), that most of the peak flows were overestimated (Fig. 3). Simulations with TMPA estimates clearly underestimated the discharge volume (around –24% of the total measured discharge volume), whereas simulations with ERA-Interim data overestimated discharge volume for the validation period (+62.56% of the total measured discharge volume); this is most probably because of the previously explained under- and overestimation of rainfall.

Table 4 Efficiency criteria for the discharge simulations (calibration period: 1999–2004, validation period: 2005–2009, full period: 1999–2009): NS, NSL and the absolute bias (VOL in %). Simulations were made with raingauge data, TMPA estimates and ERA-Interim data, as well as with the post-processed data with multiplicative shift (MS) and quantile mapping (QM). The efficiency criteria of the QM-simulations are only presented for the full period, because each year was calibrated independently.

Simulations with	Calibration			Validation			Full period		
	NS	NSL	VOL (%)	NS	NSL	VOL (%)	NS	NSL	Vol (%)
Raingauge data	0.91	0.92	−0.25	0.88	0.89	6.32	0.9	0.91	2.44
TMPA	0.52	0.74	−18.68	0.62	0.66	−24.21	0.56	0.71	−20.95
TMPA MS	0.23	0.83	10.49	0.51	0.82	8.63	0.35	0.83	9.73
TMPA QM							0.73	0.85	−3.25
ERA-Interim	0.56	0.65	−0.41	−0.11	0.42	62.56	0.34	0.55	25.36
ERA-Interim MS	0.62	0.76	−8.65	−0.39	0.68	42.89	0.19	0.72	15.98
ERA QM							0.57	0.75	−10.68

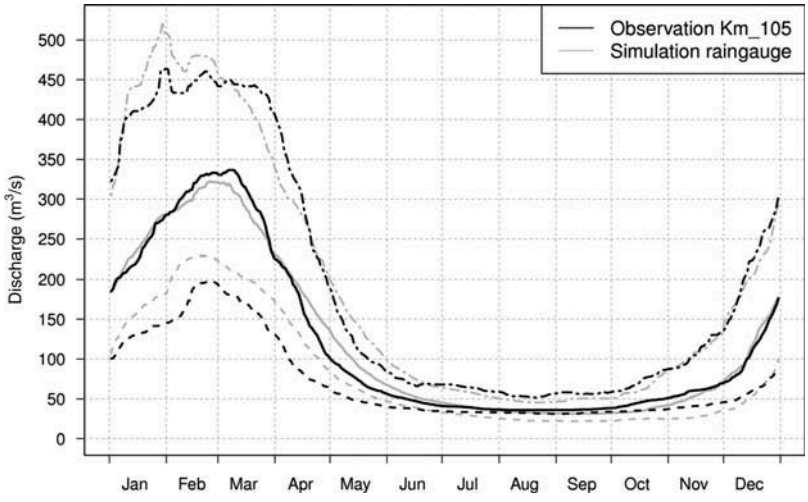

Fig. 4 Performance analysis of simulation results with raingauge data (grey lines) compared to observed data at the streamgauge station Km_105 (black lines) after calibration (1999–2009). Displayed are the 10% quantile (q10), 50% quantile (q50) and the 90% quantile (q90). The greatest discrepancies between simulated and observed discharge can be observed during months with high discharge.

Additionally, an analysis was performed to evaluate the performance of the raingauge data (Fig. 4) in reproducing higher and lower discharges. The largest discrepancies can be observed during months with high discharge; q10 und q90 are overestimated in January and February but q50 shows a generally good approximation. The model is able to reproduce the variability of discharge in the target area. In general, the comparison of the measured and simulated discharge hydrograph for the period from 1999 to 2009 indicates that the model can well simulate the total runoff and the yearly peak flows in VB.

4.2.2 After post-processing During high flows, in particular, the correction factor amplified the already high TMPA estimates and ERA-Interim data, which led to an overestimation of discharge and consequently low NS values. But apart from the high flows, the post-processing with the multiplicative shift compensated for the low TMPA and high ERA-Interim precipitation values and led to a better approximation to the measured discharge (higher NSL and smaller VOL; see Table 4).

Post-processing with quantile mapping results in much better NS, NSL and VOL values (Table 4). Since, with this method, the data range of the raingauge data was translated to the TMPA estimates and ERA-Interim data, the highest discharge values show much lower values after correction. However, compared to the measured discharge, the highest runoff values as summarized in the flow duration curve are still slightly overestimated (Fig. 3).

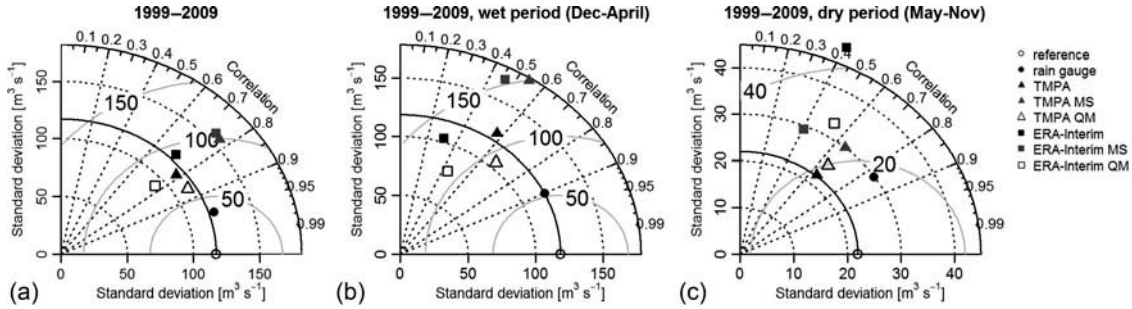

Fig. 5 Taylor diagram with standard deviation, correlation and root mean square (grey circles originating at reference) for: (a) the period 1999–2009, (b) the wet period December–April and (c) the dry period May–November. Discharge simulation with raingauge data, TMPA estimates, ERA-Interim data and the post-processed TMPA and ERA-Interim data with a multiplicative shift (MS) and quantile mapping (QM), compared with measured discharge (Km_105) as a reference.

Taylor diagrams were interpreted to see how well the simulated pattern agrees with the observed data (see Fig. 5). The Taylor diagram for 1999–2009 shows again that simulations with raingauge data yield more similar results to the reference (Km_105) than the simulations with TMPA. The correlation of simulations with the TMPA and TMPA MS is around 0.8, TMPA QM shows a slightly higher value (0.85). Simulations with ERA-Interim data (MS and QM) result with a correlation between 0.7 and 0.8. The root mean square error (marked as concentric circles originating at the reference) and standard deviation are higher for the simulations with TMPA MS and ERA-Interim MS than with the uncorrected data, which implies that they deviate from the average more and are less accurate. During the wet period (December–April), the agreement between the simulated and observed values is clearly lower than during the dry period. This also results in very low NS and NSL values for TMPA MS (e.g. December NS: –0.47, NSL: 0.17). Significantly better results can be seen during the dry period (May–November). For example, in June, NS values of 0.97 and NSL values of 0.9 were obtained for the uncorrected TMPA estimates. The ERA-Interim MS and QM approaches show a lower standard deviation and root mean square error compared to the uncorrected data.

The advantage of the quantile mapping technique is that time periods with no corresponding observed precipitation data could still be corrected with the ecdf of other time periods, where observed data exist (similarly for post-processed data with a multiplicative shift). Our results suggest that TMPA estimates and ERA-Interim data can nevertheless be considered as an additional data source in regions with sparse data, but they should not be considered as a replacement, as Scheel *et al*. (2011) also concluded. The data user should be aware of the overestimated peaks and should consider an appropriate correction technique.

4.3 Hydrological modelling of climate change scenarios

4.3.1 Monthly changes Table 5 shows the aggregated, monthly rainfall changes (ΔP) of the A1B scenario for each month of the three future time periods and GCMs. Generally, a tendency towards negative ΔP can be distinguished, which suggests there will be less rain in the future. With time, there are more negative values. The MIHR model shows the highest negative values and BMC2 the lowest. The highest negative values occur from May to August, when precipitation totals are already low; which means that the effect of the high negative values will be small. Positive ΔP values are more likely from January to April, where the values range from –16.2 to 13.9%. The ΔP of the B1 scenario shows similar values and tendencies. Under this scenario, the ΔP of the CSMK3 model is generally less extreme than for the A1B scenario.

The temperature changes (ΔT) show a clear positive tendency, which suggests temperatures will rise increasingly with time. The range of ΔT for the A1B scenario is between 0.3 and 5.6% and for the B1 scenario between –1.1 and 3.9%. The highest ΔT occurred with the MIHR model.

4.3.2 Impact on water resources in VB The impact of climate change on the daily hydrology in VB was estimated by forcing PREVAH with the application of ΔP and ΔT to the observed daily meteorological information on precipitation and

Table 5 Monthly rainfall changes (ΔP, %) for the A1B scenario.

Month	A1B scenario ΔP (%)								
	2010–2039			2040–2069			2070–2100		
	BMC2	MIHR	CSMK3	BMC2	MIHR	CSMK3	BMC2	MIHR	CSMK3
Jan	−3.0	−4.3	5.1	9.7	7.4	3.2	5.7	−0.9	−2.9
Feb	6.0	−4.6	−1.4	6.3	6.4	12.4	9.6	−1.4	−2.5
Mar	8.8	−4.9	−2.6	7.9	2.3	−4.4	7.8	6.4	−1.1
Apr	3.4	9.2	13.9	−16.2	7.1	5.3	0.8	7.7	−7.6
May	−13.0	−13.0	−35.4	9.4	−13.7	−26.4	−18.8	−15.2	−49.7
Jun	5.8	−8.6	−10.0	−10.1	−17.9	−22.6	−16.5	−43.1	−40.3
Jul	−17.1	−20.6	14.2	−25.0	−39.2	−16.5	−41.4	−45.4	−31.3
Aug	−7.5	−35.5	−14.4	−13.5	−31.7	−23.8	−13.9	−58.0	−35.8
Sep	−0.8	−2.6	15.0	−8.4	−22.2	8.5	−3.0	−39.1	7.7
Oct	−3.2	−5.8	−3.4	3.0	−17.8	−9.5	0.2	−24.8	4.7
Nov	4.2	−2.3	−1.0	1.2	−10.8	−5.7	5.7	−15.8	−12.8
Dec	−8.7	−4.4	7.3	−6.4	2.4	−7.5	−0.4	5.3	−20.6

temperature (1991–2009). By calculating the percentage change in discharge (mean of all three GCMs) and comparing our results with Lavado Casimiro *et al.* (2011), we found less negative values (Table 6). The B1 scenario in particular shows clear negative values in Lavado Casimiro *et al.* (2011), whereas our study determined mostly positive values. This could be due to the positive ΔP values at the beginning of the year (see Table 5), where the rainfall sums are already high and the effect of ΔP is therefore high. In Table 6 the months with the minimum and maximum change in discharge are displayed for the PREVAH simulations for each period. A high range can be detected. The comparison to Lavado Casimiro *et al.* (2011) is limited because of the use of two different hydrological models (MWB3, monthly time step), different observed data from two stations (Pisac and Km_105) for the baseline period, and because of the use of ΔEvaporation instead of temperature.

The outputs of the PREVAH simulations consist of various variables in the hydrological cycle that can be evaluated and used for water resources assessment, for example, (a) the total runoff (mm d^{-1}) and (b) total water in the system (mm d^{-1}) shown in Fig. 6.

The greatest changes in total runoff occur in the months with the most runoff (January–March) and for q90, with the differences likely to become much more marked in the future scenario (2069–2100). For the basin, this means that, during the rainy season, more runoff has to be expected, which could also lead to higher flood peaks. However, how great the change will finally be is uncertain as the climate models (e.g. CSMK shows lower runoff for January–March) and the scenarios A1B and B1 yield different results. These differences illustrate the uncertainties involved in modelling climate change and predicting its possible impact.

The advantage of daily simulations is that discharge fluctuations within a month can be detected, which could be important for water management. However, interpreting the simulation results on a

Table 6 Percentage of change in flow: results of simulations with hydrological models MWB3 and PREVAH. The calculated mean of the three GCMs was compared with the observed discharge: Pisac in Lavado Casimiro *et al.* (2011) and Km_105 in our study. The minimum and maximum percentage change for each period and the month when they occurred are shown in parentheses.

	A1B		B1	
	MWB3 Pisac	PREVAH Km_105	MWB3 Pisac	PREVAH Km_105
2020s	6%	2% (–8.7% Dec; 10.6% Jan)	−2%	1% (–6.5% Nov; 11.4% Jan)
2050s	3%	8% (–8.9% Nov; 25.7% Sep)	−7%	−2% (–24.8% Nov; 12.8% Sep)
2080s	−1%	6% (–30.5% Dec; 38.6% Sep)	−5%	6% (–19.7% Nov; 21.4% Aug)

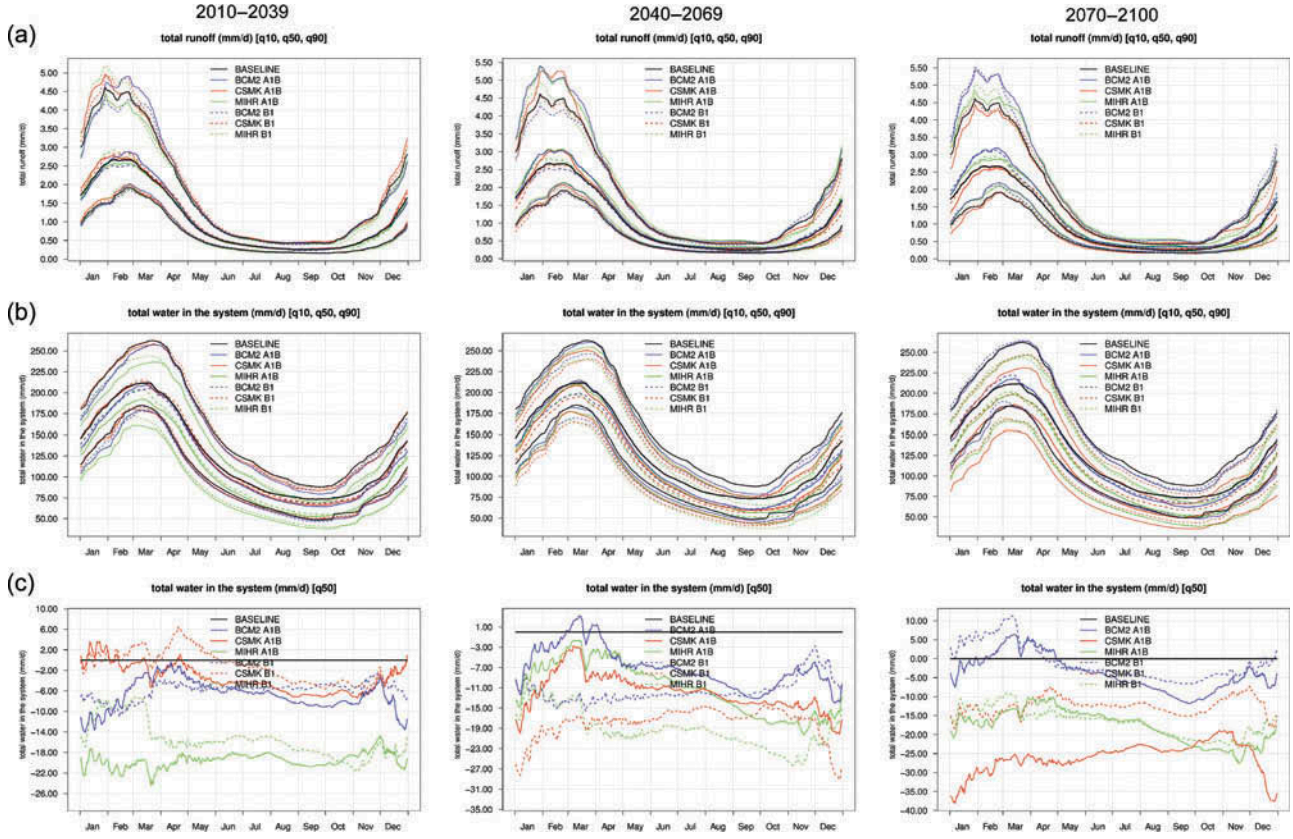

Fig. 6 Future projections of (a) total runoff and (b),(c) total water in the system (mm d^{-1}) in VB for the periods 2010–2039, 2040–2069 and 2070–2100. (c) Represents the differences to measured discharge during the baseline period (1993–2010). Total water in the system is defined as the sum of several model internal water storages: snow, interception, soil moisture, unsaturated runoff and saturated runoff. Daily PREVAH calculation results of BCM2 (blue), CSMK (red) and MIHR (green) compared with the baseline period (1993–2010) for the A1B (solid line) and B1 (dashed line) scenarios, shown for the three quantiles q10, q50 and q90; (c) only for q50). Climatology is computed by considering for each day in the year a centred moving window of 31 days.

daily scale must be done with care, since, with the Delta-change approach, we make no change in the natural variability of the meteorological input from the interpolated ground observations. It is most probable that the obtained changes within a month are smaller than the natural variability of the time series during the baseline period (see Bosshard *et al*. 2011). As a further study, a bias-correction of the GCM data could be conducted (Bosshard *et al.* 2013a).

The total water in the system in the PREVAH model (Fig. 6(b) and (c)) is defined as the sum of several model internal water storages: snow, interception, soil moisture, unsaturated runoff and saturated runoff storages (Viviroli *et al.* 2009a). In the future, less water will be temporarily stored and will thus not be available for use in the target region, which will have a great effect on the water supply, especially during the dry season. From May to November, resources are less for all GCMs and lower values are reached more often. This tendency can also be seen for the soil moisture storage for May–October and December–March, with the exception of the BCM2 model. Less water will be available for plants, which compromises agriculture. Snowmelt shows clearly lower values in the future, most likely because less snow will be stored in the target area. This will probably be most noticed during the dry season when discharge is already low. Changes in temperature will have an influence, e.g. on snow and its storage, whereas changes in precipitation have a much greater influence, e.g. on total runoff (Bosshard *et al.* 2013b). Both are dependent on the quality of the given GCM, as Ardoin-Bardin *et al.* (2009) also observed.

The difference between the baseline period and the simulation results for the multi-annual means for four water resource parameters can be distinguished in Table 7. For the baseline period, the yearly amount

Table 7 Difference (in %) between the baseline period (1993–2009) and the simulation results of multi-annual means (mm year^{-1}) for precipitation, actual evaporation, total runoff and storage of plant available soil moisture for the A1B and B1 scenarios. Negative changes are marked in bold.

	Baseline period	A1B (%)								
	1993–2009	2010–2039			2040–2069			2070–2100		
	(mm year^{-1})	BCM2	MIHR	CSMK3	BCM2	MIHR	CSMK3	BCM2	MIHR	CSMK3
Precipitation	834	0.5	**−4.2**	1.9	2.2	**−0.2**	**−0.6**	3.6	**−4.3**	**−7.3**
Actual evaporation	443	**−0.5**	**−2.0**	0.0	**−1.1**	**−3.8**	**−2.0**	**−1.1**	**−6.3**	**−3.6**
Total runoff	403	2.7	**−3.2**	5.2	9.4	10.2	3.7	14.4	8.7	**−6.0**
Soil moisture [mm]	54	0.0	**−7.4**	1.9	1.9	**−3.7**	**−3.7**	3.7	**−9.3**	**−11.1**
		B1 (%)								
Precipitation	834	**−1.8**	**−2.5**	2.5	**−2.4**	**−4.9**	**−3.7**	4.0	**−3.5**	**−0.6**
Actual evaporation	443	**−1.1**	**−3.4**	0.2	**−0.9**	**−5.6**	**−1.1**	**−0.2**	**−5.0**	**−0.2**
Total runoff	403	**−2.7**	1.5	6.0	**−3.2**	1.5	**−4.2**	9.9	5.7	2.0
Soil moisture [mm]	54	**−3.7**	**−5.6**	1.9	**−3.7**	**−9.3**	**−7.4**	3.7	**−7.4**	**−1.9**

of adjusted interpolated precipitation is around twice that of actual evaporation and of total runoff. A small part of the water is temporarily stored in the available soil moisture storage. In the future, according to the MIHR and CSMK3 models, less precipitation will occur. The tendency for actual evaporation is also negative, probably because less water is available during the dry period. The yearly mean of soil moisture will probably also decrease. Less precipitation and soil moisture will mostly affect farmers, but whether the yearly total runoff in the future will decrease or increase is not clearly detectable.

5 CONCLUSIONS

In this paper, we evaluated the use of alternative data sources for hydrological modelling of water resources in the high mountains of Peru, where few ground measurements are available. Satellite-based precipitation data (TMPA) and re-analysis data (ERA-Interim) were used for the hydrological modelling of a time period in the past in the Vilcanota basin (VB), while GCM outputs were applied for the modelling of future water resources in the region.

The TMPA estimates tended to underestimate and ERA-Interim data to overestimate the total sum of precipitation for the whole period of 1998–2009. We applied two simple post-processing methods—a multiplicative shift and quantile mapping—to correct these errors. Bias correction is a current state of research and discussion, especially for GCM correction (Ehret *et al*. 2012), but, as we demonstrated, it is also useful for other datasets like TMPA and ERA-Interim data. Generally, both post-processing methods led to a better approximation to the measured discharge. The multiplicative shift reduced the absolute bias in the TMPA estimates and ERA-Interim data, but peak flows in particular were overestimated. Quantile mapping improved the outcomes of hydrological simulations and reduced the error in higher peak flow estimates. This resulted in lower absolute bias and higher NS values. We found rain-gauge measurements more reliable for simulating total runoff than TMPA estimates and ERA-Interim data. Nevertheless, in regions with little data availability, TMPA estimates and ERA-Interim data can be considered as an important additional data source for hydrological simulations.

The newly updated TMPA 3B42 research product version 7 was released in June 2012, and includes several changes concerning the metadata, data structures, parameters and other factors. The number of output products has increased from two to six, which allows the user to better analyse and understand the information used to compute the product (Huffman *et al.* 2011). In a further investigation, it would be interesting to test the performance of this version 7 product and compare it to the results of this study.

More high-resolution satellite-based data are likely to be available in the future and re-analysis methods will improve. Therefore, further studies on the quality and availability of such satellite-based rainfall estimates and re-analysis data would be worthwhile, especially in poorly gauged areas.

For the simulation of future water resources, we applied the Delta-change method and combined the output of three GCMs with the hydrological model

PREVAH. We found changes in total runoff for months with the highest discharge (January–March), with the differences likely to become much more marked in 50 years. More runoff is to be expected during rainy season, but in total less water will be stored (e.g. as snow, interception, soil moisture, unsaturated runoff and saturated runoff storages), which could lead to water shortages, especially during dry seasons, when agriculture, fauna and humans depend on water supply the most. However, how large these changes are likely to become is uncertain, as climate models yield different results. An improvement could be made by choosing more GCMs, e.g. a higher spread in the obtained results could be expected. In particular, changes in precipitation have a marked influence, e.g. on total runoff (Bosshard *et al.* 2013b). Both precipitation and temperature are dependent on the quality of the given GCMs, as Ardoin-Bardin *et al*. (2009) also observed.

In this study, the hydrological model PREVAH was used for the first time in Peru. It seems to model the hydrological resources well and is therefore suitable for this region. The advantage of this hydrological model is the output at daily time steps. Variability within a month can be detected and used, for example, for projects in water resource management. However the results have to be interpreted with care, since, with the Delta-change method, the natural variability of the meteorological input is not changed.

We have seen that it is possible to accomplish a hydrological study of past and future water resources, even if very few data are available. Free accessible data sources, like TMPA estimates, ERA-Interim data and GCM outputs, combined with a hydrological model, provide a good basis for building a database for further studies.

Acknowledgments We thank the Ministry of Environment of Peru for enabling this study in the framework of the project PACC in Peru. Our gratitude goes to Ch. Huggel and N. Salzmann for the PACC coordination. We thank SENAMHI for providing ground measurements, the NASA/Goddard Space Flight Center (NASA/GSFC) for the TMPA data, ECMWF for the ERA-Interim data and the IPCC Distribution Centre for the GCM outputs. Further, we are grateful to M. Roher and M. Schwarb for the preparation of the data and M. Ossiaa for support in data visualization.

Funding This work was done in the framework of the project PACC, which was supported by the SDC [project number 7F-04245.09.11].

REFERENCES

Allen, M.R. and Ingram, W.J., 2002. Constraints on future changes in climate and the hydrologic cycle. *Nature*, 419 (6903), 224–232. doi:10.1038/nature01092

Ardoin-Bardin, S., *et al.*, 2009. Using general circulation model outputs to assess impacts of climate change on runoff for large hydrological catchments in West Africa. *Hydrological Sciences Journal*, 54 (1), 77–89. doi:10.1623/hysj.54.1.77

Berrisford, P., *et al*., 2009. *The ERA-Interim Archive*. ECMWF: Reading, UK. ERA Report Series, No. 1.

Bitew, M.M., *et al.*, 2012. Evaluation of high-resolution satellite rainfall products through streamflow simulation in a hydrological modeling of a small mountainous watershed in Ethiopia. *Journal of Hydrometeorology*, 13 (1), 338–350. doi:10.1175/2011JHM1292.1

Bosshard, T., *et al.*, 2011. Spectral representation of the annual cycle in the climate change signal. *Hydrology and Earth System Sciences*, 15 (9), 2777–2788. doi:10.5194/hess-15-2777-2011

Bosshard, T., *et al.*, 2013a. Quantifying uncertainty sources in an ensemble of hydrological climate-impact projections. *Water Resources Research*, 49 (3), 1523–1536. doi:10.1029/2011WR011533

Bosshard, T., *et al.*, 2013b. Hydrological climate-impact projections for the Rhine river: GCM-RCM uncertainty and separate temperature and precipitation effects. *Journal of Hydrometeorology*, 15 (2), 697–713. doi:10.1175/JHM-D-12-098.1

Bosshard, T. and Zappa, M., 2008. Regional parameter allocation and predictive uncertainty estimation of a rainfall-runoff model in the poorly gauged Three Gorges Area (PR China). *Physics and Chemistry of the Earth, Parts A/B/C*, 33 (17–18), 1095–1104. doi:10.1016/j.pce.2008.03.004

Bradley, R.S., *et al.*, 2006. Threats to water supplies in the Tropical Andes. *Science*, 312 (5781), 1755–1756. doi:10.1126/science.1128087

Buytaert, W., *et al*., 2006. Human impact on the hydrology of the Andean páramos. *Earth-Science Reviews*, 79 (1–2), 53–72. doi:10.1016/j.earscirev.2006.06.002

Buytaert, W., Célleri, R., and Timbe, L., 2009. Predicting climate change impacts on water resources in the tropical Andes: effects of GCM uncertainty. *Geophysical Research Letters*, 36, L07406. doi:10.1029/2008GL037048

Collischonn, B., Collischonn, W., and Tucci, C.E.M., 2008. Daily hydrological modeling in the Amazon basin using TRMM rainfall estimates. *Journal of Hydrology*, 360 (1–4), 207–216. doi:10.1016/j.jhydrol.2008.07.032

Dai, A., 2006. Precipitation characteristics in eighteen coupled climate models. *Journal of Climate*, 19 (18), 4605–4630. doi:10.1175/JCLI3884.1

Dee, D.P., *et al.*, 2011. The ERA-Interim reanalysis: configuration and performance of the data assimilation system. *Quarterly Journal of the Royal Meteorological Society*, 137, 553–597.

Ehret, U., *et al.*, 2012. Should we apply bias correction to global and regional climate model data? *Hydrology and Earth System Sciences*, 16 (9), 3391–3404. doi:10.5194/hess-16-3391-2012

FAO-UNESCO, 1988. *Soil map oF world, revised legend*. Rome: FAO. World Soil Resources Reports 60.

Friedl, M.A., *et al.*, 2002. Global land cover mapping from MODIS: algorithms and early results. *Remote Sensing of Environment*, 83 (1–2), 287–302. doi:10.1016/S0034-4257(02)00078-0

Gleick, P.H., 1986. Methods for evaluating the regional hydrologic impacts of global climatic changes. *Journal of Hydrology*, 88, 97–116. doi:10.1016/0022-1694(86)90199-X

Graham, L.P., *et al.*, 2007. On interpreting hydrological change from regional climate models. *Climatic Change*, 81, 97–122. doi:10.1007/s10584-006-9217-0

Gurtz, J., *et al.*, 2003. A comparative study in modelling runoff and its components in two mountainous catchments. *Hydrological Processes*, 17 (2), 297–311. doi:10.1002/hyp.1125

Huffman, G.J., *et al.*, 2007. The TRMM Multi-satellite Precipitation Analysis (TMPA): Quasiglobal, multiyear, combined sensor precipitation estimates at fine scales. *Journal of Hydrometeorology*, 8 (1), 38–55. doi:10.1175/JHM560.1

Huffman, G.J., *et al.*, 2011. Highlights of Version 7 TRMM Multi-satellite Precipitation Analysis (TMPA). *In*: C. Klepp and G.J. Huffman, eds. *5th International Preciptation Working Group Workshop, Workshop Program and Proceedings*, 11–15 October 2010, Hamburg: Max-Planck-Institut für Meteorologie, 109–110. Reports on Earth System Science.

INEI, 2011. *Sistema de información regional para la toma de decisiones SIRTOD* [online]. Lima, Peru: INEI. Available from: http://www.inei.gob.pe/ [Accessed 1 March 2013].

IPCC (Intergovernmental Panel on Climate Change), 2001a. *Climate change 2001: Impacts, adaptation and vulnerability*. Contribution of Working Group II to the Third Assessment Report of the Intergovernmental Panel on Climate Change. J.J. McCarthy, *et al*., eds. Cambridge, UK: Cambridge University Press, 1032.

IPCC (Intergovernmental Panel on Climate Change), 2001b. *Climate change 2001: The scientific basis*. Contribution of Working Group I to the Third Assessment Report of the Intergovernmental Panel on Climate Change. J.T. Houghton, *et al*., eds. Cambridge, UK: Cambridge University Press, 881.

IPCC (Intergovernmental Panel on Climate Change), 2007. *Climate change 2007: Impacts, adaptation and vulnerability*. Contribution of Working Group II to the Fourth Assessment Report of the Intergovernmental Panel on Climate Change. M.L Parry, *et al*., eds. Cambridge, UK: Cambridge University Press, 976.

Jakob Themeßl, M., Gobiet, A., and Leuprecht, A., 2011. Empirical-statistical downscaling and error correction of daily precipitation from regional climate models. *International Journal of Climatology*, 31 (10), 1530–1544. doi:10.1002/joc.2168

Jiménez, K.Q., Collischonn, W., and Lavado, C. W. S., 2011. Modelización hidrológica usando estimaciones de lluvia por satélite en la cuenca del río Huallaga, Perú. *Revista Peruana Geo-Atmosférica RPGA*, 3, 51–62.

Kobierska, F., *et al.*, 2013. Future runoff from a partly glacierized watershed in Central Switzerland: a two-model approach. *Advances in Water Resources*, 55, 204–214. doi:10.1016/j.advwatres.2012.07.024

Koboltschnig, G.R., *et al.*, 2008. Runoff modelling of the glacierized Alpine Upper Salzach basin (Austria): multi-criteria result validation. *Hydrological Processes*, 22 (19), 3950–3964. doi:10.1002/hyp.7112

Laghari, A.N., Vanham, D., and Rauch, W., 2012. To what extent does climate change result in a shift in Alpine hydrology? A case study in the Austrian Alps. *Hydrological Sciences Journal*, 57 (1), 103–117. doi:10.1080/02626667.2011.637040

Lavado Casimiro, W.S., *et al.*, 2009. TRMM rainfall data estimation over the Peruvian Amazon-Andes basin and its assimilation into monthly water balance models. *In*: K.K. Yilmaz, *et al*., ed. *New approaches to hydrological prediction in data-sparse regions*, September. Oxfordshire: International Association of Hydrological Sciences, IAHS Publ, 333, 245–252.

Lavado Casimiro, W.S., *et al.*, 2011. Assessment of climate change impacts on the hydrology of the Peruvian Amazon–Andes basin. *Hydrological Processes*, 25, 3721–3734. doi:10.1002/hyp.8097

Lavado Casimiro, W.S., *et al.*, 2012. Trends in rainfall and temperature in the Peruvian Amazon–Andes basin over the last 40 years (1965–2007). *Hydrological Processes*, doi:10.1002/hyp.9418

Lavado Casimiro, W.S., Silvestre, E., and Pulache, W., 2010. Tendencias en los extremos de lluvias cerca a la ciudad del Cusco y su relación con las inundaciones de enero del 2010. *Revista Peruana Geo-Atmosférica RPGA*, 2, 89–98.

Lorenz, C. and Kunstmann, H., 2012. The hydrological cycle in three state-of-the-art reanalyses: intercomparison and performance analysis. *Journal of Hydrometeorology*, 13 (5), 1397–1420. doi:10.1175/JHM-D-11-088.1

Menzel, L., 1996. Modelling canopy resistances and transpiration of grassland. *Physics and Chemistry of the Earth*, 21 (3), 123–129. doi:10.1016/S0079-1946(97)85572-3

Oliver, M.A. and Webster, R., 1990. Kriging: a method of interpolation for geographical information systems. *International journal of geographical information systems*, 4 (3), 313–332. doi:10.1080/02693799008941549

Oltchev, A., *et al*., 2002. The response of the water fluxes of the boreal forest region at the Volga's source area to climatic and land-use changes. *Physics and Chemistry of the Earth, Parts A/B/C*, 27, 675–690. doi:10.1016/S1474-7065(02)00052-9

Pan, M., Li, H., and Wood, E., 2010. Assessing the skill of satellite-based precipitation estimates in hydrologic applications. *Water Resources Research*, 46, W09535. doi:10.1029/2009WR008290

Panofsky, H.A. and Brier, G.W., 1968. *Some applications of statistics to meteorology*. Philadelphia: The Pennsylvania State University Press.

Randall, D.A., *et al.*, 2007. Climate models and their evaluation. *In*: S. Solomon, *et al*., eds. *Climate change 2007: the physical science basis*. Contribution of working group I to the fourth assessment report of the Intergovernmental Panel on Climate Change. New York, NY: Cambridge University Press.

Randin, C.F., *et al.*, 2009. Climate change and plant distribution: local models predict high-elevation persistence. *Global Change Biology*, 15 (6), 1557–1569. doi:10.1111/j.1365-2486.2008.01766.x

Salzmann, N., *et al.*, 2009. Integrated assessment and adaptation to climate change impacts in the Peruvian Andes. *Advances in Geosciences*, 22, 35–39. doi:10.5194/adgeo-22-35-2009

Sánchez-Vega, I. and Dillon, M.O., 2006. Jalcas. *In*: R. M. Moraes, *et al*., eds. *Botánica Económica de los Andes Centrales*. La Paz, Bolivia: Herbario Nacional de Bolivia, Instituto de Ecología, Universidad Mayor de San Andrés, 77–90.

Scheel, M.L.M., *et al.*, 2011. Evaluation of TRMM Multi-satellite Precipitation Analysis (TMPA) performance in the Central Andes region and its dependency on spatial and temporal resolution. *Hydrology and Earth System Sciences*, 15 (8), 2649–2663. doi:10.5194/hess-15-2649-2011

Schwarb, M., *et al.*, 2011. A data portal for regional climatic trend analysis in a Peruvian High Andes region. *Advances in Science & Research*, 6, 219–226. doi:10.5194/asr-6-219-2011

Semenov, M.A. and Stratonovitch, P., 2010. Use of multi-model ensembles from global climate models for assessment of climate change impacts. *Climate Research*, 41 (1), 1–14. doi:10.3354/cr00836

Su, F., Hong, Y., and Lettenmaier, D.P., 2008. Evaluation of TRMM Multisatellite Precipitation Analysis (TMPA) and its utility in hydrologic prediction in the La Plata Basin. *Journal of Hydrometeorology*, 9 (4), 622–640. doi:10.1175/2007JHM944.1

Taylor, K.E., 2001. Summarizing multiple aspects of model performance in a single diagram. *Journal of Geophysical Research-Atmospheres*, 106 (D7), 7183–7192. doi:10.1029/2000JD900719

Tobin, K.J. and Bennett, M.E., 2010. Adjusting satellite precipitation data to facilitate hydrologic modeling. *Journal of Hydrometeorology*, 11 (4), 966–978. doi:10.1175/2010JHM1206.1

Vergara, W., *et al.*, 2011. *Assessment of the impacts of climate change on mountain hydrology. Development of a methodology through a case study in the Andes of Peru*. Washington, DC: The World Bank.

Villar, J.C.E., *et al.*, 2009. Spatio-temporal rainfall variability in the Amazon basin countries (Brazil, Peru, Bolivia, Colombia, and Ecuador). *International Journal of Climatology*, 29 (11), 1574–1594. doi:10.1002/joc.1791

Viviroli, D., *et al.*, 2009a. An introduction to the hydrological modelling system PREVAH and its pre- and post-processing-tools. *Environmental Modelling & Software*, 24 (10), 1209–1222. doi:10.1016/j.envsoft.2009.04.001

Viviroli, D., *et al.*, 2009b. Continuous simulation for flood estimation in ungauged mesoscale catchments of Switzerland - Part I: Modelling framework and calibration results. *Journal of Hydrology*, 377 (1–2), 191–207. doi:10.1016/j.jhydrol.2009.08.023

Viviroli, D., *et al.*, 2011. Climate change and mountain water resources: overview and recommendations for research, management and policy. *Hydrology and Earth System Sciences*, 15, 471–504. doi:10.5194/hess-15-471-2011

Viviroli, D., Gurtz, J., and Zappa, M., 2007. *The hydrological modelling system PREVAH. Model documentation and user manual*. Berne: Geographica Bernensia P40, Department of Geography, University of Berne.

Wagner, S., *et al*., 2009. Water balance estimation of a poorly gauged catchment in West Africa using dynamically downscaled meteorological fields and remote sensing information. *Physics and Chemistry of the Earth, Parts A/B/C*, 34 (4–5), 225–235. doi:10.1016/j.pce.2008.04.002

Zappa, M. 2002. *Multiple-response verification of a distributed hydrological model at different spatial scales*. Dissertation (Dissertation). ETH Zürich.

Zappa, M., *et al.*, 2003. Seasonal water balance of an Alpine catchment as evaluated by different methods for spatially distributed snowmelt modelling. *Nordic Hydrology*, 34 (3), 179–202.

Zappa, M. and Gurtz, J., 2003. Simulation of soil moisture and evapotranspiration in a soil profile during the 1999 MAP-Riviera Campaign. *Hydrology and Earth System Sciences*, 7 (6), 903–919. doi:10.5194/hess-7-903-2003

Zappa, M. and Kan, C., 2007. Extreme heat and runoff extremes in the Swiss Alps. *Natural Hazards and Earth System Sciences*, 7 (3), 375–389. doi:10.5194/nhess-7-375-2007